JOURNAL OF CATALYSIS 114, 388–397 (1988)

Nickel and Molybdenum Sulfides Loaded into Zeolites: Activity for Catalytic Hydrogenation

J. LEGLISE, A. JANIN, J. C. LAVALLEY, AND D. CORNET[1]

Laboratoire Catalyse et Spectrochimie, UA CNRS 04.0414, I.S.M.Ra, Université de Caen, 14032 Caen Cedex, France

Received August 7, 1987; revised April 28, 1988

Stabilized HY zeolites containing nickel or molybdenum, or the combination Ni–Mo, as well as a dealuminated zeolite containing Ni–Mo, were submitted to sulfiding. The ability of these solids to catalyze benzene hydrogenation was tested. The sulfide phases in the zeolites were further characterized by their capacity for oxygen and carbon monoxide chemisorptions, and by infrared spectra of adsorbed CO. Sulfidation of Mo or Ni–Mo in the zeolites is incomplete, ranging from 50 to 90%. Lowest sulfur levels are observed after reacting unsaturated hydrocarbons under a high hydrogen pressure. Activity for benzene hydrogenation is a sensitive test of the catalytic properties and suggests the formation of a NiMoS phase inside the zeolite. The synergy observed between Ni and Mo is confirmed by the appearance of a band at 2086 cm^{-1} in the IR spectrum of adsorbed CO. Side reactions are also observed in the course of benzene conversion. Extra-lattice aluminum favors selectivity toward hydrogenation.

INTRODUCTION

Modern hydrocracking catalysts are required to have a flexible selectivity combined with high activity. This may be achieved by associating a zeolite (*1–4*) with a hydrogenation catalyst. Transition metal sulfides (TMS) such as pure or supported Ni–Mo–S (*5–8*) are effective hydrogenation catalysts and meet the requirements of resistance toward N and S poisons. They are indeed frequently cited in hydroprocessing formulas. Although the TMS are not specifically inserted into the zeolite component of the actual catalysts, it is relatively easy to introduce Ni and Mo ions in an acidic zeolite. Then it appears to be feasible to perform sulforeduction, and hence to obtain a Ni–Mo sulfide encaged in the zeolite.

Literature concerning TMS-containing zeolites is scarce (*9–16*). Richardson (*9*) showed that benzene hydrogenation catalyzed by nickel in Y zeolites was strongly poisoned by sulfur compounds and that the remaining activity was correlated with unsulfided nickel. However, Döhler (*10*) mentioned that Ni–Mo and Ni–W sulfides in HY zeolites were promising catalysts for upgrading coal-derived middle distillates. Many papers are devoted to hydrodesulfurization (*11–16*) catalyzed by faujasites and mordenites. For this process, Cid *et al.* (*11*) reported a synergy between Co and Mo in a NaY zeolite. The appearance of a NiMoS phase was also claimed by Davidova *et al.* (*12*). In many cases, the zeolite catalysts were reduced before sulfiding (*12–16*).

We investigated here a strongly acidic material, a stabilized HY zeolite, which was doped with nickel or molybdenum, or a combination of both. The material was then sulfided, and the ability of the TMS to catalyze hydrogenation was assessed by reacting benzene, with special attention being focused on the synergy between Ni and Mo. The hydrogenation test was carried out under steady sulfiding conditions and under high pressure, close to those used in industrial practice. Since synergies between Ni and Mo sulfides usually vary from one support to another, the possible influence of

[1] To whom correspondence should be addressed.

0021-9517/88 $3.00

extra-lattice aluminium on the properties of the TMS was also studied. The TMS were further characterized by means of oxygen and carbon monoxide chemisorptions, and by FTIR of adsorbed CO, as a check of dispersion and promotion of the sulfide phase.

EXPERIMENTAL

1. *Materials*

The starting material was a stabilized zeolite Y supplied by Linde (Ref. LZY 82), containing 0.15% sodium and 2.8% ammonium by weight. It is hereafter named SY. Chemical analysis revealed that the overall silicon-to-aluminium atomic ratio amounted to 2.7. The cell parameter of the ammoniated solid is 2.456 nm and shrinks to 2.451 nm after being calcined at 773 K. The reported surface area of the calcined material is 770 m^2g^{-1}. Cationic aluminium species do exist in the SY zeolite since the number of framework aluminium atoms calculated from Na^+ and NH_4^+ charge balancing ($\approx$24 Al/u.c.) is definitely smaller than the total number of Al ($\approx$52/u.c. from chemical analysis). For that reason, a dealuminated HY carrier, SDY, was prepared by treating SY with a 1 *M* HCl solution. The overall Si/Al atomic ratio rose to 4.5 in the SDY material. The γ-alumina support used for comparative purposes was GFS-C from Rhône-Poulenc (surface area 240 m^2g^{-1}).

2. *Chemicals and Gases*

High-purity (>99.5%) reagents benzene, *n*-heptane, and dimethyldisulfide (DMDS) were from Prolabo. The gases, hydrogen, hydrogen sulfide, oxygen, carbon monoxide, helium, and argon, were from Air Liquide. They were freed from impurities by standard methods, except H_2S which was used without further purification.

3. *Catalysts*

Nickel was introduced into the zeolite by ion exchange at room temperature from a 0.4 *M* nickel acetate solution (pH 6.7). The loading could not exceed 60% of the ammonium content of SY. The maximum nickel content was 6.8 ions per zeolite unit cell for the starting SY and 4.8 ions for the dealuminated SDY. Most of the residual sodium was eliminated during the exchange process.

Molybdenum was loaded either by the incipient wetness impregnation method with a 0.4 *M* $Mo_7O_{24}(NH_4)_6$ solution at a pH of 6 (Mo/SY and NiMo/SY) or by condensation of $Mo(CO)_6$ vapor at room temperature (NiMo/SDY). For NiMo/zeolites, nickel was introduced before molybdenum.

The main chemical features of the nickel and molybdenum samples studied here are summarized in Table 1. The metal contents were determined using atomic absorption, and sulfur contents were measured by coulometric titration after burning off the sulfided solids at 1600 K. Surface areas measured after calcination at 773 K were 535 m^2g^{-1} (Ni and NiMo/SY) and 508 m^2g^{-1} (Mo/SY). Crystallinities from XRD (*17*) varied from 80% (SY) to 61% (NiMo/SY) and 52% (Mo/SY).

The Ni and Mo/Al_2O_3 preparations have been previously described (*18*, *19*). The NiMo/Al_2O_3 is a commercial catalyst, HR 346 from Procatalyse.

4. *Catalytic Activity Measurements*

(*a*) *High-pressure reactor and catalyst pretreatments*. The flow system was de-

TABLE 1

Chemical Characterization of the Zeolite- and Alumina-Based Catalysts

Catalyst designation	NiO (wt%)	MoO_3 (wt%)	Ni + Mo total metal loading (mol kg^{-1})	Ni/(Ni + Mo) (mol ratio)
Ni/SY	4.25	—	0.57	1
Mo/SY	—	12.1	0.83	0
NiMo/SY	3.27	12.6	1.32	0.33
NiMo/SDY	2.9	4.65	0.71	0.52
Ni/Al_2O_3	3.6	—	0.48	1
Mo/Al_2O_3	—	14.0	0.97	0
NiMo/Al_2O_3	3.5	14.0	1.44	0.32

Note. Metal weights are related to solid samples calcined under O_2 flow at 773 K.

signed to work under a total pressure of 8 MPa. An amount of pelleted catalyst (W = 0.180 g, grain size 0.16–0.20 mm) diluted with silicon carbide was placed in a vertical tubular reactor (12 mm i.d.) made of stainless steel (SS 316). The hydrocarbon reagents were introduced with a microfeed liquid pump at a rate of 0.2 $cm^3\ h^{-1}$ and vaporized instantly when mixed with the hydrogen flow (4.8 liters h^{-1}). The void parts of the system were minimized to reduce the observed time response.

The reactor could be swept by oxygen or argon to allow calcination of the catalyst at 1 atm. Then, a hydrogen pressure of 8 MPa was established to perform catalyst sulfidation. The catalysts were sulfided with a mixture of *n*-heptane (78 wt%) + benzene (20%) + DMDS (2%). The temperature was progressively raised (1 K min^{-1}) to 593 K and was then kept constant for 24 h.

(*b*) *Benzene reaction.* The reactor temperature was lowered to 440 K before switching to a new reactant mixture: benzene (98 wt%) + DMDS (2%). DMDS was completely decomposed at all catalyst temperatures above 473 K, so that the H_2/H_2S molar ratio was kept higher than 2000. The reactor temperature and benzene flow rate F_b^0 being chosen, the hydrogen flow rate was adjusted to obtain the desired benzene pressure P_b^0. The effluent was analyzed by on-line gas chromatography, using OV-101 and OV-1701 capillary columns. The hydrogenation conversion was defined as

$$x_h = \frac{\text{moles of MCP and CHx}}{\text{moles of benzene at inlet}},$$

where MCP and CHx stand for methylcyclopentane and cyclohexane, respectively. Alkylaromatics and cracked products were also detected and their specific conversions determined as above. No significant aging deactivation was found after operating the catalyst for 1 month. The sulfur contents of the zeolites were determined after each run.

The "sulfidation extent" reported in Table 2 is conventionally taken as 100% if full transformation into Ni_3S_2 and MoS_2 occurs. Such a composition is commonly reported for alumina-supported catalysts (*20*).

5. *Dynamic Chemisorption Measurements*

The gas uptakes were measured according to a pulse technique described elsewhere (*18*). The pretreatment procedure carried out at atmospheric pressure involved sulfiding the zeolite at 593 K either with a H_2–H_2S mixture (12 mol% H_2S), or with a H_2–H_2S–CH_4 mixture (10 mol% H_2S) provided by decomposition of DMDS in a separate reactor. Sulfur contents (Table 2) were determined at this stage, and also after performing chemisorptions.

The carbon monoxide uptakes, N_{CO}, were measured at 273 K and the oxygen uptakes, N_O, at 333 K, the carrier gas being argon. Oxygen titration followed that of carbon monoxide. Between the two succes-

TABLE 2

Extent of Sulfidation of Unused and Used Ni and Mo Catalysts

Sulfiding procedure[a]			Reaction	Sulfidation extent S/($\frac{2}{3}$ Ni + 2 Mo) (mol ratio)				
Gas mixture	Total pressure (MPa)	H_2/H_2S (mol ratio)		Ni/SY	Mo/SY	NiMo/SY	NiMo/SDY	$NiMo/Al_2O_3$
$H_2 + H_2S + CH_4$	0.1	10	No	1.02	0.57	0.50	0.87	0.84
$H_2 + H_2S$	0.1	7.5	Chemisorption	1.07	0.58	0.56	0.94	0.92
H_2 + *n*-C_7 + Be + DMDS	8	2700	Benzene	0.71	0.30	0.50	0.72	0.58

[a] Sulfiding temperature was 593 K.

sive titrations, the catalyst surface was cleaned of chemisorbed CO by heating at 473 K for 20 min. We checked that oxygen titration of the sulfide made directly or after CO titration led to very close results for Mo and $NiMo/Al_2O_3$ catalysts.

6. *Infrared Measurements*

The solid samples were self-supported disks ($\approx$10 mg cm^{-2}) compressed at 200 MPa. The spectra were recorded with a Nicolet MX-1 spectrometer. Sulfidations of the preoxidized and evacuated samples were performed directly at 593 K with three successive batches of a H_2S (10 mol%)–H_2 mixture at an equilibrium pressure of 13 kPa. The first two batches contacted the solids for 1 h and the third one for 12 h. CO adsorption was investigated at different CO pressures, 1.3 and 33 kPa, and dynamic 1 mPa. The latter gave the so-called "irreversible" CO bands.

RESULTS AND DISCUSSION

1. *Sulfidation of the Ni–Mo Zeolites*

The sulfur contents of the catalysts which have been kept working for 1 month under a high hydrogen pressure are shown in the third row of Table 2. They are distinctly lower than those of the catalysts which were sulfided at atmospheric pressure (rows 1 and 2). A similar observation was reported for $NiMo/Al_2O_3$ catalysts (*21*). It appears that the sulfur contents depend mainly on the H_2S/H_2 ratio, which is highest when sulfiding is performed at 1 atm. Under these conditions, the stoichiometry of the nickel sulfide in Ni zeolites was beyond Ni_3S_2 but the buildup of the Mo or Ni–Mo sulfide was incomplete. Attempts to obtain a deeper sulfidation by raising the temperature to 700 K were unsuccessful. Moreover, predecomposition of DMDS was about equivalent to direct introduction of H_2S (rows 1 and 2).

In any case, sulfiding the NiMo/SY under high pressure achieved only 50% conversion of the transition metals into sulfides. The sulfur stoichiometry of the Ni–Mo combination supported on the dealuminated zeolite SDY was higher. Interestingly, it was about the same as that on the alumina support (last column of Table 2).

2. *Benzene Hydrogenation*

The benzene hydrogenation test performed under high pressure is appropriate for comparing catalysts using a zeolite or an alumina carrier. On most catalysts, the main reaction observed at 593 K was benzene hydrogenation into cyclohexane and methylcyclopentane. Figure 1 shows the variation of the degree of conversion, x_h, with the reciprocal flow rate, W/F_b^0, in a series of experiments performed on the NiMo/SY catalyst at constant benzene pressure. The linear parts of such plots yield the hydrogenation rates, R_h. The data collected in Table 3 were obtained at 593 K with benzene flow rates such that W/F_b^0 was less than 0.1 kg h mol^{-1}. Under these conditions, hydrogenation conversions x_h were kept below 0.07. The MCP/CHx ratio observed on zeolite catalysts was around 9, exceeding the equilibrium value 5.5 (*22*),

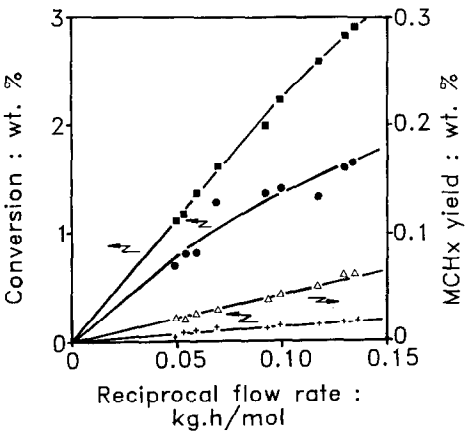

FIG. 1. Conversion degree of benzene into various products versus reciprocal flow rate for NiMo/SY catalyst (587 K, P_b^0 = 50 kPa, total pressure 8 MPa). (■) Methylcyclopentane and cyclohexane. (●) Alkylaromatics. (+) Pentane and isopentane. (△) Methylcyclohexane.

TABLE 3

Benzene Conversion over Sulfided Catalysts

Catalyst	Hydrogenation[a] conversion (wt%)	Alkylation[a] conversion (wt%)	Hydrogenation rate constant k_b (mol h^{-1} kg^{-1})	k_b/([Ni] + [Mo]) (h^{-1})	E_a (kJ mol^{-1})
Ni/SY	0.20	0.09	0.025	0.044	78
Mo/SY	0.65	0.17	0.076	0.091	78
NiMo/SY	2.8	2.55	0.320	0.25	76
NiMo/SDY	1.14	3.10	0.135	0.19	77
NiMo/Al_2O_3	6.8	<0.07	0.800	0.56	55

[a] Data collected for reaction temperature = 593 K; P_b^0 = 70 kPa; total pressure = 8 MPa; W/F_b^0 = 0.085 kg h mol^{-1}.

while cyclohexane was selectively formed over the alumina-based HR 346.

Many other products were found with the zeolite catalysts. The main side-product was toluene but it was accompanied by some C_8-alkylaromatics, the toluene-to-C_8 ratio being about 2 at 593 K. These alkylaromatics could arise from a reaction between benzene and DMDS or some of its decomposition products. From the values of the conversions of benzene into alkylaromatics, shown in Fig. 1 and Table 3, the importance of the process may be assessed. Alkylation was practically nil with the NiMo/Al_2O_3 catalyst, showing that it was a heterogeneous and acid-catalyzed process. It was most important with the NiMo deposited onto the SY and the SDY carriers. On these two catalysts, 3.3% of the benzene underwent alkylation: this is close to the value expected if all of the DMDS was used up in the process. Even so, a large quantity of methane was produced, indicating that hydrogenolysis of DMDS was not the only cause of alkylation.

Finally, small amounts of C_7 and higher naphthenes were also detected at the highest reaction temperatures ($T > 580$ K). For instance, the amounts of methylcyclohexane are shown in Fig. 1. These naphthenes probably result from secondary hydrogenation of the already-mentioned alkylaromatics. The appearance of light alkanes in the C_3–C_5 range also indicates some naphthene degradation at the highest temperature but coke formation remained very low.

The dependence of the reaction rates upon partial pressure at constant flow rate is illustrated in Fig. 2. For benzene pressures higher than 25 kPa, the hydrogenation rate was constant, meaning that the surface was saturated with strongly absorbed benzene. Thus, all activities reported for the sulfide catalysts were measured at P_b^0 above 25 kPa and the initial reaction rates are expressed in Table 3 as zero-order rate con-

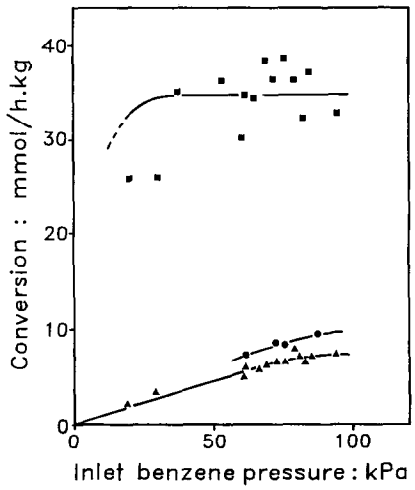

FIG. 2. Rate of benzene conversion (mol h^{-1} kg^{-1}) versus benzene inlet pressure for Mo/SY (560 K, total pressure 8 MPa, W/F_b^0 = 0.08 kg h mol^{-1}). (■) Conversion into MCP and CHx. (●) Alkylaromatics. (▲) Toluene.

stants, k_b, for the zeolites as well as for the $NiMo/Al_2O_3$ catalyst. The ratio H_2/H_2S, varying in the range 2000–5000, had no definite influence upon the measured rates. The rate of toluene formation on the contrary increased with reactant partial pressure. Under these conditions, the alkylation rate followed an apparent first-order law.

Apparent activation energies for hydrogenation on the different catalysts are reported in Table 3. The values measured were in line with those reported for similar systems (*9, 23, 24*). All zeolite catalysts exhibited an activation energy higher than the $NiMo/Al_2O_3$, so that the activity differences between catalysts supported on alumina and zeolite decreased with increasing temperature. Moreover, the activation energy did not vary much with the metal loaded onto the zeolite or with the amount of extra-framework aluminium species.

Comparison of the activities for hydrogenation allows a clear distinction between the catalysts. The intrinsic activities k_b/([Ni] + [Mo]) (Table 3) vary in the order

$$NiMo/Al_2O_3 > NiMo/SY \quad \text{or} \quad SDY > Mo/SY > Ni/SY.$$

Thus, the NiMoS phase was more active for benzene hydrogenation on the alumina carrier than in the zeolites. A similar observation was reported for reduced nickel (*9*). In addition, the activity of our $NiMo/Al_2O_3$ catalyst was close to that found by Sapre and Gates (*25*) for a $CoMo/Al_2O_3$ catalyst performing the same reaction under similar conditions.

For the catalysts based on zeolite SY, a synergy appeared between nickel and molybdenum since the intrinsic activity of molybdenum was amplified by a factor of 4.1 when nickel was present. This, however, does not prove that the Ni–Mo combination obtained in the zeolites has the same optimal synergy as that found on alumina. Indeed, the overall sulfur stoichiometry of the NiMo/SY catalyst was lower than that of the $NiMo/Al_2O_3$ catalysts (Table 2).

In fact, the Ni/Si and Mo/Si ratios measured by XPS on the sulfided zeolites (*26*) showed that the metal concentrations were about the same at the surface of the grains as in the bulk. The high dispersion of molybdenum was already noted in the case of NaY impregnated with heptamolybdate (*27*). Thus, the "NiMoS" phase is located inside the zeolite grains, so that the active phase is not as accessible to the hydrocarbon reagents in a zeolite as it is on alumina.

There are, however, some analogies between the alumina- and zeolite-based catalysts. In both cases, molybdenum sulfide is more active than nickel sulfide for hydrogenation. Furthermore, the intrinsic activity (per metal atom) of NiMo/SY which contains some extra-lattice aluminium is slightly higher than for NiMo/SDY.

The nature of the support is more decisive toward the selectivity for benzene transformation. Alkylation, secondary hydrogenation, isomerization, and cracking appeared as side-reactions on the zeolite catalysts. For zeolites containing a single metal, molybdenum was both more active and more selective than nickel for hydrogenation. The NiMo zeolites, which are the most active, are also the least selective. Since the sulfided NiMo zeolites are not expected to be much more acidic than the monometallic samples, it is likely that the zeolite promotes two different alkylation processes: one is acid-catalyzed and involves decomposition of DMDS, the second is related to hydrogenolysis of C–C bonds and requires a bifunctional catalyst under high hydrogen pressure.

Moreover, the large amount of methylcyclopentane in the hydrogenated products means that the C_6 ring underwent isomerization into C_5 before all hydrogenation steps were completed (*28*). This behavior is a feature of a bifunctional catalyst in which the acidic function prevails over the hydrogenation function. The latter is indeed rather sensitive to the procedure followed in the sulfidation step (*20*).

TABLE 4

Chemisorption Data and Turnover Frequencies for Ni and Mo Catalysts

Catalyst	Oxygen chemisorption		Carbon monoxide chemisorption		TOF (h^{-1}) Benzene hyd.
	N_O (mol at. kg^{-1})	N_O/Me[a]	N_{CO} (mol kg^{-1})	N_{CO}/Me[a]	
Ni/SY	0.039	0.068	0.044	0.077	0.65
Ni/Al_2O_3	0.039	0.080	0.001	0.002	—
Mo/SY	0.076	0.092	0.021	0.025	0.84
Mo/Al_2O_3	0.172	0.177	0.007	0.007	—
NiMo/SY	0.108	0.082	0.063	0.048	3.2
NiMo/SDY	0.056	0.079	0.031	0.044	2.4
$NiMo/Al_2O_3$	0.270	0.187	0.023	0.017	3.0

[a] Me is the active metal concentration (mol kg^{-1}) (see Table 1).

2. *Chemisorption of CO and Oxygen*

The results of benzene hydrogenation suggested that the metallic sulfide encaged in the Y zeolites differs from the NiMoS phase encountered on $NiMo/Al_2O_3$ catalyst by a slightly lower activity and a higher activation energy. Dynamic chemisorption measurements involving carbon monoxide and oxygen were performed to evaluate the number of surface sites on both types of catalyst. The measurements were carried out at temperatures identical to those used by Bachelier *et al.* (*29*) for alumina-supported sulfides. Nevertheless, the CO or O_2 uptakes over alumina-supported catalysts depend to a large extent upon the sulfidation procedure (*30*). Hence, we shall compare the data obtained on catalysts sulfided under similar conditions.

The relevant data are collected in Table 4. The bare support SY took up negligible quantities of CO (less than 3 mmol kg^{-1}) and no oxygen at all. Thus, the chemisorptions are characteristic of the metal introduced.

In all cases, it appeared that the zeolite catalysts chemisorbed more CO and less oxygen than the corresponding alumina-supported sulfides.

It is thought that the oxygen takeup is primarily related to the extent of sulfidation of supported nickel and molybdenum ions. This is illustrated by Fig. 3, which refers to catalysts sulfided at atmospheric pressure with a high H_2S/H_2 ratio. Oxygen uptake, N_O, increases with the sulfur content, determined after the chemisorption measurement. At 593 K, molybdenum encaged in the zeolites underwent incomplete sulfidation. As suggested by the N_O values as well as the sulfur contents (Table 2), adding Ni and Mo in the zeolite does not facilitate the sulfidation as it does on the alumina carrier.

CO chemisorption on alumina-supported catalysts is specific for the sulfide phase

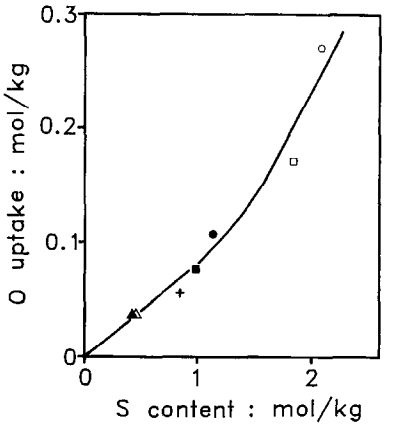

FIG. 3. Oxygen uptakes, N_O (mol of O atoms kg^{-1}), versus sulfur contents of the catalysts. (□) Mo/Al_2O_3; (■) Mo/SY. (△) Ni/Al_2O_3; (▲) Ni/SY. (○) $NiMo/Al_2O_3$; (●) NiMo/SY; (+) NiMo/SDY.

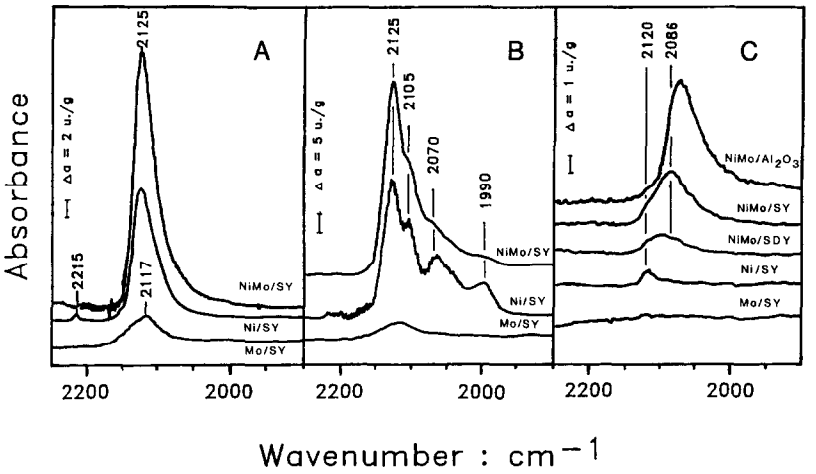

FIG. 4. Infrared absorption spectra of CO adsorbed on sulfided catalysts (gas-phase spectrum substracted). (A) P_{CO} = 1.3 kPa; (B) P_{CO} = 33 kPa; (C) After CO evacuation, P_{CO} = 1 mPa.

and affords a count of hydrogenolysis sites (*31, 32*). For zeolites containing Mo or Ni, CO probably reaches nonsulfided metal ions in addition to the sulfide phase. The corresponding metal–carbonyl complexes are stabilized by the zeolite support since N_{CO} values were much higher in this case than for Mo/Al_2O_3 and Ni/Al_2O_3. Similarly, in the NiMo zeolites the complete sulfidation was not achieved, and CO reaches both sulfided and nonsulfided metal ions. However, no correlation between N_{CO} and hydrogenation rate was apparent.

Furthermore, contrary to the NiMo or $CoMo/Al_2O_3$ catalysts with a low Mo content (*31, 32*), the CO uptakes by the NiMo/ zeolites were nearly the sums of the individual contributions expected for Ni and Mo, so that there was no synergetic effect according to this criterion.

The N_O values measured on the NiMo zeolites are related to the amount of NiMoS phase. One may ask whether the number of catalytic sites involved in hydrogenation is related to N_O as was observed for CoMo/ Al_2O_3 (*33*). To check this, we calculated turnover frequencies (TOF) by dividing hydrogenation rates by N_O. Results appear in Table 4. For benzene hydrogenation, the turnovers for the NiMo zeolites were clearly higher than those for the monometallic zeolites and close to that for NiMo/ Al_2O_3. This provides some support for the formation of a mixed NiMoS phase occurring inside the zeolite channels.

3. *Infrared Spectra of Adsorbed CO*

The vibrational frequency of CO adsorbed onto the sulfide catalysts provides an excellent clue to the formation of a mixed CoMoS phase in alumina-supported catalysts (*32*). The method was applied here to confirm the formation of a mixed sulfided phase dispersed in the HY zeolites.

The absorption spectra recorded in the 1900–2300 cm^{-1} range are reported in Figs. 4A and 4B for CO equilibrium pressures equal to 1.3 and 33 kPa (the spectrum of the gas phase has been substracted), whereas the species remaining adsorbed after evacuation are shown in Fig. 4C.

The Mo/SY zeolite exhibited a rather broad and asymmetric band with a maximum at 2117 cm^{-1}. This wavenumber was slightly higher (about 10 cm^{-1}) than that for a sulfided Mo/Al_2O_3 catalyst (*32, 34*). The band observed on the Mo/SY zeolite disappeared upon evacuation; it can be attributed to a low-valent molybdenum atom belonging to a sulfide phase. In addition to

this main species, other kinds of Mo species are suspected from the high-frequency edge of the band, revealing the occurrence of Mo ions in an intermediate oxidation state since a Mo^{4+}–CO complex would absorb at 2190 cm^{-1} (*35*).

The Ni/SY zeolite yielded simple spectra only at low CO pressure. The main feature of the spectrum under these conditions was a strong band at 2125 cm^{-1}, which did not completely disappear upon evacuation. By comparison, a sulfided Ni/Al_2O_3 catalyst exhibits a reversible CO band at 2080 cm^{-1} attributed to reduced Ni ions belonging to a sulfide phase (*36*). The band at 2125 cm^{-1} over the sulfided Ni/SY sample is more reminiscent of the carbonyl species observed by Kermarec *et al.* (*37*) with mildly reduced NiX zeolites: the absorption occurring at 2120 cm^{-1} on this sample was attributed to a $Ni^+(CO)$ complex. The absorption at 2125 cm^{-1} observed here on sulfided Ni/SY is attributed to the same monocarbonyl species, since a weak band occurred at the same position for the nonsulfided Ni/SY (*38*). In Ref. (*37*), a second carbonyl complex was detected over the reduced Ni*X* sample, with absorptions at 2105 and 2145 cm^{-1}. These are characteristic of a dicarbonyl species $Ni^+(CO)_2$. Accordingly, raising the CO pressure over the sulfided Ni/SY sample (Fig. 4B) led to one new band at 2105 cm^{-1}. The asymmetric vibration expected at 2145 cm^{-1} for the corresponding $Ni^+(CO)_2$ species is not evidenced. However, this band should be of low intensity, according to the "metal–surface selection rule" (*39*); thus, it can be overlapped by the strong band at 2125 cm^{-1}.

The appearance of the Ni^+–CO complexes over the Ni/SY sample which underwent sulforeduction may be attributed to Ni ions which are partly reduced but probably not sulfided. Moreover, the weak band appearing at 2215 cm^{-1} (Fig. 4A) reveals that some Ni^{2+} ions (*40*) were not affected by the sulfidation procedure. Additional bands at 2070 and 1990 cm^{-1} indicate the presence of nickel tetracarbonyl in an adsorbed state (also detected in the gas phase), and possibly of other CO complexes of zero-valent Ni (*40*). Thus, according to the CO probe, the sulfided Ni/SY zeolite has a variety of nickel sites, some of which do not belong to a sulfide entity.

The spectra recorded for the NiMo/SY and NiMo/SDY samples were qualitatively similar to those for the Ni/SY samples. The main feature of Fig. 4 was again a band at 2125 cm^{-1} ascribed as before to a $Ni^+(CO)$ complex. A pressure increase to 33 kPa also generated $Ni^+(CO)_2$ complexes, but the amount of adsorbed $Ni(CO)_4$ was much lower than that for Ni/SY. Most interesting was the effect of evacuation (Fig. 4C): an intense and rather broad absorption persisted, with a maximum at 2086 cm^{-1} and a shoulder at 2120 cm^{-1}. Although the maximum at 2086 cm^{-1} was not strictly identical with that observed on sulfided $NiMo/Al_2O_3$ (2079 cm^{-1}), it is likely that similar NiMoS phases are formed in both supports. This explains the enhanced activity observed for benzene hydrogenation. However, this promoted phase does not involve all of the nickel contained in the zeolite because the "irreversible" CO band at 2120 cm^{-1} reveals Ni^+ ions which are not combined with molybdenum. The CO dynamic chemisorption data also suggested that some of the nickel ions were not included into the mixed phase.

CONCLUSION

Summarizing the results obtained by different techniques, we showed that nickel and molybdenum introduced in a zeolite were able to combine into a mixed NiMo sulfide phase with apparent dispersion and catalytic hydrogenation properties close to those of the well-known NiMoS phase supported on alumina. Transformation into sulfide, however, is incomplete, as shown by the low sulfur content, particularly on the SY zeolite, but removal of extra-aluminum species favors the sulfide formation. The mixed sulfide phase obtained in zeolites has

a good hydrogenation capacity toward benzene, but lower than that on alumina. The presence of aluminium species in the zeolite channels favors selectively the hydrogenation. Secondary reactions due to the acidic properties are important. The method of oxygen chemisorption is helpful in measuring the amount of active sulfide and correlates roughly with the rate of benzene hydrogenation. On the contary, CO chemisorption is not specific for the hydrogenation catalytic sites of these zeolite materials.

ACKNOWLEDGMENTS

This work was supported by the French Délégation Générale à la Recherche Scientifique et Technique. The authors are grateful to Dr. A. Chambellan for help in the design of the high pressure system, and to Mrs. M. Marzin for technical assistance.

REFERENCES

1. Gladrow, E. M., and Parker, P. T., Brit. Patent 913,923 (1962).
2. Myers, C. G., Rope, B. W., and Garwood, W. E., U.S. Patent 3,384,572 (1968).
3. Kittrell, J. R., U.S. Patent 3,558,471 (1971).
4. Child, E. T., and Messing, D. A., U.S. Patent 3,562,144 (1971).
5. Vaughan, D. E. W., *in* "The Properties and Applications of Zeolites" (Townsend, R. P., Ed.)., Chem. Soc. Spec. Publ. Vol. 33, p. 294. 1980.
6. Chianelli, R. R., *Catal. Rev. Sci. Eng.* **26,** 361 (1984).
7. Topsøe, H., and Clausen, B. S., *Catal. Rev. Sci. Eng.* **26,** 395 (1984).
8. Yermakov, Yu. I., *Russ. Chem. Rev.* **55,** 499 (1986).
9. Richardson, J. T., *J. Catal.* **21,** 122 (1971).
10. Döhler, W., "Proceedings, 8th International Congress on Catalysis, Berlin, 1984," Vol. III, p. 499. Verlag Chemie, Weinheim, 1984.
11. Cid, R., Orellana, F., and López-Agudo, A., *Appl. Catal.* **32,** 327 (1987).
12. Davidova, N., Kovacheva, P., and Shopov, D., "Stud. Surf. Sci. and Catal. Series," Vol. 24, p. 659. Elsevier, Amsterdam, 1985.
13. Echevskii, G. V., and Ione, K. G., "Stud. Surf. Sci. and Catal. Series," Vol. 5, p. 273. Elsevier, Amsterdam, 1980.
14. Sugokia, M., and Aomura, K., *Prepr. Amer. Chem. Soc. Div. Pet. Chem. Symp.* **25,** 245 (1980).
15. Brooks, C. S., *Surf. Technol.* **10,** 379 (1980).
16. Kallo, D., Onyestyak, G., and Papp, J., Jr., "Proceedings, 6th Int. Zeol. Conf., Reno, 1983" (D. Olson and A. Bisio, Eds.). p. 444. Butterworths, London, 1984.
17. A.S.T.M. D.3906-80, Philadelphia, PA, 1980.
18. Bachelier, J., Duchet, J. C., and Cornet, D., *J. Phys. Chem.* **84,** 15 (1980).
19. Bachelier, J., Tilliette, M. J., Duchet, J. C., and Cornet, D., *J. Catal.* **76,** 300 (1982).
20. Bachelier, J., Tilliette, M. J., Duchet, J. C., and Cornet, D., *J. Catal.* **87,** 292 (1984).
21. Chambellan, A., Delahaie, S., Cornet, D., and Hémidy, J. F., *Appl. Catal.* **34,** 181 (1987).
22. *Amer. Pet. Inst. Res. Proj.* **44** (1949–1987).
23. Voorhoeve, R. J. H., and Stuiver, J. C. M., *J. Catal.* **23,** 228 (1971).
24. Somorjai, G. A., *in* "Chemistry in Two Dimensions: Surfaces," p. 448. Cornell Univ. Press, Ithaca, NY, 1981, and refs. therein.
25. Sapre, A. V., and Gates, B. C., *Ind. Eng. Chem. Prod. Res. Dev.* **20,** 68 (1981).
26. Mériaudcau, P., results to be published.
27. Fierro, J. L. G., Conesa, J. C., and López-Agudo, A., *J. Catal.* **108,** 334 (1987).
28. Weisser, O., and Landa, S., "Sulphide Catalysts, Their Properties and Applications," p. 81. Academia, Prague, 1972.
29. Bachelier, J., Duchet, J. C., and Cornet, D., *Bull. Soc. Chim. Belg.* **90,** 1301 (1981).
30. Vissers, J. P. R., Bachelier, J., Ten Doeschate, H. J. M., Duchet, J. C., De Beer, V. H. J., and Prins, R. "Proceedings, 8th International Congress on Catalysis, Berlin, 1984," Vol. II, p. 387. Verlag Chemie, Weinheim, 1984.
31. Bachelier, J., Duchet, J. C., and Cornet, D., *J. Catal.* **87,** 283 (1984).
32. Bachelier, J., Tilliette, M. J., Cornac, M., Duchet, J. C., Lavalley, J. C., and Cornet, D., *Bull. Soc. Chim. Belg.* **93,** 743 (1984).
33. Zmierczak, W., Muralidhar, G., and Massoth, F. E., *J. Catal.* **77,** 432 (1982).
34. Peri, J. B., *J. Phys. Chem.* **86,** 1615 (1982).
35. Millman, W. S., Crespin, M., Cirillo, A. C., Abdo, S., and Hall, W. K., *J. Catal.* **60,** 404 (1978).
36. Ouafi, D., Thesis, Caen, 1986.
37. Kermarec, M., Olivier, D., Richard, M., Che, M., and Bozon-Verduaz, F., *J. Phys. Chem.* **86,** 2818 (1982).
38. Cornac, M., Thesis, Caen, 1986.
39. Pearce, H. A., and Sheppard, N., *Surf. Sci.* **59,** 205 (1976).
40. Peri, J. B., *J. Catal.* **86,** 84 (1984).